



# High-redshift Galaxies from Early JWST Observations: Constraints on Dark Energy Models

N. Menci<sup>1</sup>, M. Castellano<sup>1</sup>, P. Santini<sup>1</sup>, E. Merlin<sup>1</sup>, A. Fontana<sup>1</sup>, and F. Shankar<sup>2</sup>

<sup>1</sup>INAF—Osservatorio Astronomico di Roma, via Frascati 33, I-00078 Monte Porzio, Italy; [nicola.menci@inaf.it](mailto:nicola.menci@inaf.it)

<sup>2</sup>School of Physics & Astronomy, University of Southampton, Highfield, Southampton SO17 1BJ, UK

Received 2022 August 24; revised 2022 September 16; accepted 2022 September 27; published 2022 October 12

## Abstract

Early observations with JWST have led to the discovery of an unexpectedly large density (stellar-mass density  $\rho_* \approx 10^6 M_\odot \text{Mpc}^{-3}$ ) of massive galaxies (stellar masses  $M_* \geq 10^{10.5} M_\odot$ ) at extremely high redshifts  $z \approx 10$ . While such a result is based on early measurements that are still affected by uncertainties currently under consideration by several observational groups, its confirmation would have a strong impact on cosmology. Here we show that—under the most conservative assumptions and independently of the baryon physics involved in galaxy formation—such galaxy abundance is not only in tension with the standard  $\Lambda$ CDM cosmology but provides extremely tight constraints on the expansion history of the universe and on the growth factors corresponding to a wide class of Dynamical Dark Energy (DDE) models. Adopting a parameterization  $w = w_0 + w_a(1 - a)$  for the evolution of the DDE equation of the state parameter  $w$  with the expansion factor  $a$ , we derive constraints on combinations of  $(w_0, w_a)$  that rule out with confidence level  $>2\sigma$  a major portion of the parameter space  $(w_0, w_a)$  allowed (or even favored) by existing cosmological probes.

*Unified Astronomy Thesaurus concepts:* [Cosmological parameters \(339\)](#); [High-redshift galaxies \(734\)](#); [Galaxy evolution \(594\)](#)

## 1. Introduction


The abundance of massive galaxies at high redshifts constitutes a powerful probe for cosmological models. In fact, in the standard Cold Dark Matter (CDM) scenario (see Peebles 1993) the exponential high-mass tail of the mass function of dark matter (DM) halos is expected to shift toward progressively smaller masses for increasing redshift (see, e.g., Del Popolo & Yesilyurt 2007 for a review) at a rate that depends on the assumed cosmology. Hence, the comparison of the predicted abundance of massive DM halos at increasingly larger redshift with the observed abundance of galaxies with corresponding stellar mass  $M_*$  provides increasingly strong constraints on the assumed cosmological framework. The critical issue in the comparison is the translation from a predicted number density  $N(M, z)$  of DM halos with mass  $M$  to a prediction for the abundance of galaxies with stellar mass  $M_*$ . In fact, the relation between  $M$  and  $M_*$  depends on the complex physics of baryons involved in galaxy formation. However, very robust constraints can be derived under the (extremely) conservative assumption that the stellar mass corresponds to that of all the available baryons contained in a given DM halos  $M_* = (\Omega_b/\Omega_m)M \equiv f_b M$ , where  $f_b$  is the cosmic baryon fraction. In fact, for any observed stellar mass  $M_*$ , assuming smaller  $M_*/M$  ratios would yield a larger DM mass  $M$  and hence lower predicted abundance. Thus, given an observed number density  $N_{\text{obs}}(M_*, z)$  at redshift  $z$ , the condition  $N(M_*/f_b, z) \geq N_{\text{obs}}(M_*, z)$  provides a robust and extremely conservative constraint on the halo-mass function (and hence on cosmology), which is independent of the actual baryon physics relating  $M_*$  and  $M$ . Such approach has been adopted in

Menci et al. (2020) to constrain Dynamical Dark Energy (DDE) models from different observations concerning the abundance of massive galaxies at redshifts  $z = 3-6$ , and recently by Boylan-Kolchin (2022) and Lovell et al. (2022) to the abundance of massive galaxies measured from the James Webb Space Telescope (JWST) NIRCam observations of the Cosmic Evolution Early Release Science (CEERS) program (Labbe et al. 2022). While calibration issues and uncertainties related to the assumed initial mass function (IMF) are still under debate, confirmation of such JWST measurements would imply that the high-mass end of the mass function evolves surprisingly little from  $z \approx 10$  to  $z \approx 6$ , yielding a high stellar-mass density  $\rho_* \approx 10^6 M_\odot \text{Mpc}^{-3}$  at  $z = 10$ , which is in strong tension with the faster evolution predicted by  $\Lambda$ CDM. Here we apply the above approach to show that the observed CEERS abundance is actually in tension with a wide class of cosmological models. Adopting for the DE equation of state parameter  $w$  the form  $w = w_0 + w_a(1 - a)$  (introduced by Chevallier–Polarski–Linder; Chevallier & Polarski 2001; Linder 2003) employed in most DE studies, we derive strong constraints on the combinations  $(w_0, w_a)$ . These have been shown to capture the dynamics of a wide class of scalar field DE models (for the mapping of such a parameterization onto physical DE, see, e.g., Caldwell & Linder 2005; Linder 2006; Scherrer 2015; Sangwan et al. 2018), although such a parameterization fails to describe the dynamics of some DE models, like those characterized by the rapid, step-like transition of  $w$  at  $z \leq 2$  (see Linden & Virey 2008).

## 2. Method

We adopt the Sheth & Tormen (1999) mass function

$$\frac{dN}{dM} = \frac{A \bar{p}}{M^2} \frac{d \ln \nu}{d \ln M} \left( \frac{1}{\bar{v}^{2q}} + 1 \right) \frac{\bar{v}^2}{\pi} e^{-\bar{v}^2/2}, \quad (1)$$

 Original content from this work may be used under the terms of the [Creative Commons Attribution 4.0 licence](#). Any further distribution of this work must maintain attribution to the author(s) and the title of the work, journal citation and DOI.

where  $\bar{\rho}$  is the background average density;  $\nu = \delta_c / \sigma(M, z)$ , where  $\delta_c$  corresponds to the critical linear overdensity for collapse; and  $\sigma(M, z)$  is the variance of the linear density field smoothed on the scale  $R = [3M/4\pi\bar{\rho}]^{1/3}$  and evolving with time according to the linear growth factor  $D(z)$  of density perturbations. We assume a CDM form for the linear power spectrum (consistent with the measurements from the cosmic microwave background, CMB; see Planck Collaboration et al. 2020). The parameters  $a = 0.71$  and  $q = 0.3$  are related to the physics of collapse and  $\bar{\nu} = \sqrt{a}\nu$ . The normalization factor is  $A = 0.32$ .

The motivations for adopting the above form of the mass function are the following: (1) Among the different proposed forms (see Jenkins et al. 2001; Warren et al. 2006; Tinker et al. 2008) since the seminal paper by Press & Schechter (1974), this is the expression that provides the most extended high-mass tail and thus constitutes the most conservative form for our scopes. (2) Theoretical works (Sheth & Tormen 1999; Maggiore & Riotto 2010; Corasaniti & Achitouv 2011; Achitouv & Corasaniti 2012) have shown that its form is physically motivated in terms of the collapse process of halos. (3) The Sheth & Tormen (1999) form has been tested against  $N$ -body simulations for a variety of CDM cosmologies. These include the cases of a critical universe, of an open universe, and the  $\Lambda$ CDM case. Achitouv et al. (2014) studied the mass function in the Peebles & Ratra (1988) quintessence model of DE, finding that the parameters defining the key quantities determining the coefficients  $q$  and  $a$  change by less than 5% when passing from  $\Lambda$ CDM to the quintessence cosmology for large masses  $M \geq 10^{11} M_\odot$  relevant to this paper. Despali et al. (2016) have tested the above mass function against the SBARBINE set of  $N$ -body simulations for a variety of combinations of  $\Omega_m$  (ranging from 0.2 to 0.4) and  $\Omega_\Lambda$  (ranging from 0.6 to 0.8). These authors concluded that—with the proper definition of halo—the Sheth & Tormen (1999) mass function is universal as a function of redshift and cosmology to within 20%, an uncertainty that we consider in our analysis. As for the threshold  $\delta_c$ , we notice that in principle this depends weakly on cosmology. Here we shall adopt the conservative value  $\delta_c = 1.65$  for all DDE models. This constitutes a lower bound for the possible values taken in different DDE cosmologies (Mainini et al. 2003; Pace et al. 2010), thus maximizing the predicted abundance of DM halos.

The exponential cutoff in Equation (1) is critically determined by the cosmic expansion rate and by the growth factor  $D(z)$ , which depend on the equation of state of DE,  $w(a) = w_0 + w_a(1 - a)$ . In the above parameterization, the standard  $\Lambda$ CDM cosmology corresponds to  $w_0 = -1$  and  $w_a = 0$ . The cosmic expansion rate  $H(z)$  and cosmic volume  $V_{w_0, w_a}(z)$  depend on  $w_0$  and  $w_a$  as recalled in Menci et al. (2020). As for the growth factor  $D(z)$ , we use the parameterization to the solutions given in Linder (2005) and reported in Menci et al. (2020). This reproduces the behavior of the growth factor to within 0.1%–0.5% accuracy for a wide variety of DDE cosmologies (Linder 2005; Linder & Cahn 2007) and allows for a rapid scanning of the parameter space of DDE models. We normalize the amplitude of the linear power spectrum in terms of  $\sigma_8$ , the local ( $z=0$ ) variance of the density field smoothed over regions of  $8 h^{-1}$  Mpc. Present cosmological constraints based on Planck data, baryonic acoustic oscillations, and Type Ia supernovae yield  $\sigma_8 \approx 0.8$  for the  $\Lambda$ CDM cosmology; such a value varies by  $\approx 2\%$  when different

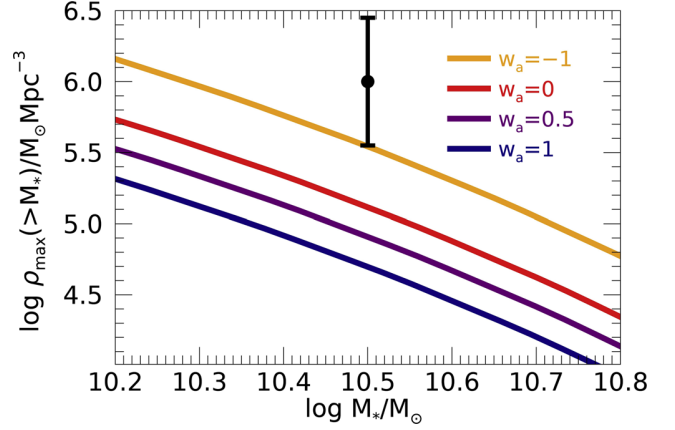


**Figure 1.** The maximal stellar-mass density predicted by DDE scenarios with  $w_0 = -1$  and four different values of  $w_a$  shown in the legend. In the predictions, we have considered an uncertainty of 0.5 dex in the value of  $M_*$ . The point is the value measured by Labbe et al. (2022). For the sake of simplicity, the latter—derived assuming a  $\Lambda$ CDM cosmology—has not been rescaled to the different values corresponding to different cosmological scenarios (see text).

combinations ( $w_0, w_a$ ) are assumed (Ade et al. 2016; Di Valentino et al. 2017; Mehrabi 2018). To adopt a conservative approach, so as to maximize the predicted abundance of large-mass DM halos, we adopt the value  $\sigma_8 = 0.83$ .

### 3. Results

Here we compare the maximal stellar-mass densities  $\rho_{\max, w_0, w_a}(>M_*)$  allowed by different combinations ( $w_0, w_a$ ) with the values  $\rho_{\text{obs}}(>M_*)$  measured by Labbe et al. (2022). We focus on the most massive bin considered by the above authors corresponding to  $M_* \geq \overline{M_*} = 10^{10.5} M_\odot$  in the redshift range  $z_1 = 9 \leq z \leq z_2 = 11$ , corresponding to a cosmic volume  $V(z_1, z_2)$ . The corresponding predicted maximal (i.e., assuming  $M = \overline{M_*}/f_b$ ) stellar-mass density,

$$\rho_{\max}(>\overline{M_*}) \equiv \int_{z_1}^{z_2} \int_{\overline{M_*}}^{\infty} \frac{dN}{dM} f_b M dM \frac{dV}{dz} \frac{dz}{V(z_1, z_2)}, \quad (2)$$

is shown in Figure 1 for DDE cosmologies with fixed  $w_0 = -1$  and four different values of  $w_a$ , and compared with the measurement by Labbe et al. (2022) from the early JWST observations.

To derive robust conservative upper limits, we assumed the most conservative value for  $f_b$ , which is still consistent with CMB observations. For the Planck values (Planck Collaboration et al. 2020)  $\Omega_b h^2 = 0.0224 \pm 0.0001$ ,  $h \equiv H_0/100 \text{ km s Mpc}^{-1} = 0.674 \pm 0.05$ , and  $\Omega_m = 0.315 \pm 0.007$ , we derive  $f_b = 0.18$  as the most conservative estimate (this upper limit holds also for CMB measurements in DDE cosmologies; see Ade et al. 2016). In addition, in Figure 1 the predictions for  $\log \rho_{\max}$  from Equation (2) include the 20% theoretical uncertainty on the mass function recalled in Section 2. This has been considered as an error bar of 0.08 dex on the predictions for  $\log \rho_{\max}$  computed from Equation (2), and the predictions are conservatively computed at the upper tip of such an error bar.

The  $\Lambda$ CDM case ( $w_a = 0$ ) is well below the  $1\sigma$  deviation from the observational value  $\rho_{\text{obs}}$  and thus in tension (at the  $\approx 2\sigma$  level) with observations as obtained by Boylan-Kolchin (2022). Notice that our prediction in the  $\Lambda$ CDM case is slightly

larger than that obtained by Boylan-Kolchin (2022) due to our consideration of measurement uncertainties in the observed value of  $M_*$  and to our conservative choice of adopting  $f_b = 0.18$ , while the latter author adopts  $f_b = 0.158$ , derived from the best-fit values of the Planck cosmological parameters. The tension is larger for increasing values of  $w_a$ , thus showing that the condition  $\rho_{\max}(>M_*) \geq \rho_{\text{obs}}(>M_*)$  provides extremely stringent constraints on DDE models.

To explore the impact of the measured stellar-mass density on the full parameter space of DDE models and derive the proper confidence level for exclusion for each considered cosmology, we consider a grid of DDE models characterized by different combinations  $(w_0, w_a)$ . For each combination, we first correct the observed densities  $\rho_{\text{obs}}$  with the volume factor  $f_{\text{Vol}} = V_{\Lambda}/V_{w_0, w_a}$  (computed in the redshift range  $z = 9 - 11$ ) to account for the fact that the volume density given in Labbe et al. (2022) has been derived assuming a  $\Lambda$ CDM cosmology. Analogously, we must take into account that the stellar masses measured by the above authors have been inferred from luminosities assuming a  $\Lambda$ CDM cosmology to convert observed fluxes into luminosities. Thus, for each combination  $(w_0, w_a)$ , we must correct the measured masses by a factor of  $f_{\text{lum}} = D_{L, w_0, w_1}^2 / D_{L, \Lambda}^2$ , where  $D_{L, w_0, w_1}$  is the luminosity distance at  $z = 10$  for the considered  $(w_0, w_a)$  combination and  $D_{L, \Lambda}$  is its value in the  $\Lambda$ CDM case. For each combination  $(w_0, w_a)$ , we compare the (cosmology corrected) observed mass density of galaxies  $\rho_{\text{obs}}(>\overline{M}_*)$  at  $z = 10$  with the predicted maximal density  $\rho_{\max, w_0, w_a}(>\overline{M}_*)$  corresponding to each  $(w_0, w_a)$  combination.

The confidence for the exclusion of each considered DDE model is obtained as the probability that  $\rho_{\text{obs}}(>\overline{M}_*) > \rho_{\max, w_0, w_a}(>\overline{M}_*)$ . The probability of measuring a given value is derived through a Monte Carlo procedure based on the average value and variance given by the observed point and error bars in Labbe et al. (2022). To be conservative, we assign an error bar of 0.5 dex to the measured stellar mass to account for systematic related to the spectral energy distribution (SED) fitting procedure (see Santini et al. 2015). In our Monte Carlo procedure, the limit stellar mass  $\overline{M}_*$  is extracted in such an interval after a flat distribution to simulate systematic uncertainties. The resulting exclusion regions in the parameter space  $(w_0, w_a)$  are shown in Figure 2 for different confidence levels and compared with regions allowed by existing probes.

The  $\Lambda$ CDM case is excluded at almost the  $2\sigma$  level, while a major fraction of the parameter space is excluded with a high confidence level. The exclusion region is overplotted on the regions allowed by CMB and weak-lensing constraints and on the region derived by the combination of the same data with the Hubble diagram of supernovae and distant quasars (Risaliti & Lusso 2019). Our probe severely restricts the region in DDE parameter space allowed by other methods and excludes almost all of the regions favored by the distant quasar method.

#### 4. Discussion and Conclusions

Our results show the potential impressive impact of JWST observations of distant galaxies on cosmology. The measurements of the abundance of galaxies at very high redshifts within the reach of JWST indeed constitute a cosmological probe competitive with the existing canonical probes. We stress that, on the computational side, our results are extremely conservative and robust with respect to existing uncertainties, as we summarize below.

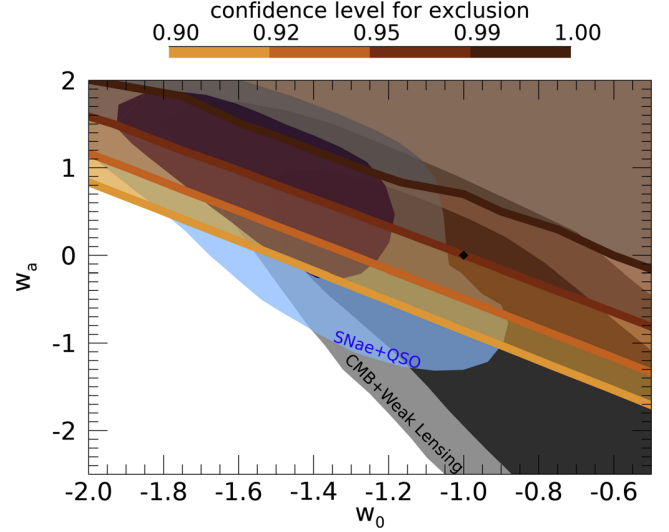


**Figure 2.** Exclusion regions in the  $w_0$ - $w_a$  plane derived from the observed stellar-mass density at  $z = 10$  (Labbe et al. 2022). The regions above each colored line correspond to exclusion with the confidence levels shown in the upper bar. Our exclusion region is compared with the  $2\sigma$  and  $3\sigma$  contours allowed by CMB+weak lensing (gray and dark-gray regions) and by the combination of the same data with the Hubble diagram of supernovae and quasars (blue regions), derived from Figure 4 of Risaliti & Lusso (2019). The black dot corresponds to the  $\Lambda$ CDM case ( $w_0 = -1, w_a = 0$ ).

1. The results do not depend on the physics of baryons involved in galaxy formation. Indeed, they have been derived under the extreme assumption that all baryons are in the form of stars.
2. We adopt the Sheth & Tormen halo-mass function. Among the different forms proposed so far, this is the one that provides the more extended tail at high masses and may even overestimate the abundance of massive halos (Wang et al. 2022).
3. Independence from the filter choice and the form of DM. We adopt a CDM spectrum (Bardeen et al. 1986; Hlozek et al. 2012). However, on the large mass scales  $M \geq 10^{10} M_{\odot}$  considered, here the variance  $\sigma(M)$  is in practice independent of the filter function used to relate it to the power spectrum (see Benson et al. 2013) and of the free-streaming properties of DM.
4. Conservative choice of cosmological parameters. For the normalization of the spectrum, we adopt  $\sigma_8 = 0.83$ , the upper limit allowed by Planck even considering alternative cosmologies (see Di Valentino et al. 2017; Mehrabi 2018), thus maximizing the predicted number of massive halos. For  $h, \Omega_m$ , and  $\Omega_b$  we considered the combination that, within the uncertainties, allows for the largest baryon fraction  $f_b = 0.18$ .
5. For the collapse threshold  $\delta_c$ , we chose the lower limit  $\delta_c = 1.65$  within the range allowed by DDE models, again maximizing the abundance of massive halos.
6. We allowed for an additional uncertainty of 0.5 dex on the measured value  $\overline{M}_*$ . This again constitutes a conservative assumption. Uncertainties related to the SED-fitting procedure reported in Labbe et al. (2022) correspond to values  $\approx 0.2$  dex.

While our conclusions are robust on the theoretical side, critical issues may affect the observational measurements we compare with. For example, potential uncertainties may affect

the calibration of the JWST photometric data used by Labbé et al. (2022). Regrettably, there is not a firm assessment of the NIRCam calibrations, which may still be subject to revision to the level of 10%–20%, especially in the short-wavelength bands (Boyer et al. 2022). At face value, the aforementioned uncertainty is not expected to yield revisions of the  $M/L$  ratios of the targets large enough to affect significantly our conclusions. A first test of the effects of the calibration revision using the independent GLASS-JWST-ERS sample (Treu et al. 2022) showed that on average, stellar masses are affected to a level of  $\approx 0.2$  dex. However, we caution that the effect on the overall shape of the galaxy SED (as well as the assumptions on the star formation histories adopted in the SED-fitting procedure; Ryan et al. 2022) may reflect in a nonlinear way on the estimated physical parameters of some objects. A second issue may concern the Chabrier IMF adopted by Labbé et al. (2022) to derive stellar masses. While assuming other universal forms for the IMF based on low-redshift conditions would not change (or even make stronger) the constraints we derive, the star formation process can be significantly different at the high redshifts. In particular, the increase of gas temperatures in star-forming, high-redshift galaxies (also contributed by the heating due to CMB photons) could result in an increasing contribution of massive stars to the galactic light, which would yield significantly lower values for the stellar masses (the exact value depending on the assumed gas temperature) compared to those measured by Labbé et al. (2022); see Steinhardt et al. (2022).

Our comprehensive statistical analysis reported in Figure 2 highlights that only extreme DDE models, with very specific combinations of  $w_0$  and  $w_a$ , may still be marginally consistent with existing cosmological probes. In addition, our results suggest that almost all baryons must be in the form of stars at high redshifts  $z \approx 9$ –10. The corresponding low gas fractions would lead to profound implications for hydrogen reionization owing to the expected large escape fractions, at least within the galactic stellar-mass range probed in this work.

#### ORCID iDs

N. Menci  <https://orcid.org/0000-0002-4096-2680>  
 M. Castellano  <https://orcid.org/0000-0001-9875-8263>  
 P. Santini  <https://orcid.org/0000-0002-9334-8705>  
 E. Merlin  <https://orcid.org/0000-0001-6870-8900>  
 A. Fontana  <https://orcid.org/0000-0003-3820-2823>

F. Shankar  <https://orcid.org/0000-0001-8973-5051>

#### References

- Lovell, C. C., Harrison, I., Haricane, Y., Tacchella, S., & Wilkins, M. 2022, arXiv:2208.10479
- Achitouv, I. E., & Corasaniti, P. S. 2012, *JCAP*, 02, 002
- Achitouv, I., Wagner, C., Weller, J., et al. 2014, *JCAP*, 2014, 077
- Ade, P. A. R., Aghanim, N., Planck Collaboration, et al. 2016, *A&A*, 594, A14
- Bardeen, J. M., Bond, J. R., Kaiser, N., & Szalay, A. S. 1986, *ApJ*, 304, 15
- Benson, A. J., Farahi, A., Cole, S., et al. 2013, *MNRAS*, 428, 1774
- Boyer, M. L., Anderson, J., Gennaro, M., et al. 2022, *RNAAS*, 6, 191
- Boylan-Kolchin, M. 2022, arXiv:2208.01611
- Caldwell, R. R., & Linder, E. V. 2005, *PhRvL*, 95, 141301
- Chevallier, M., & Polarski, D. 2001, *IJMPD*, 10, 213
- Corasaniti, P. S., & Achitouv, I. 2011, *PhRvD*, 84, 023009
- Del Popolo, A., & Yesilyurt, I. S. 2007, *ARep*, 51, 709
- Despali, G., Giocoli, R. E., Angulo, R. E., et al. 2016, *MNRAS*, 456, 2486
- Di Valentino, E., Melchiorri, A., Linder, E. V., & Silk, J. 2017, *PhRv*, 100, 103520
- Hlozek, R., Dunkley, J., Addison, G., et al. 2012, *ApJ*, 749, 90
- Jenkins, A., Frenk, C. S., White, S. D. M., et al. 2001, *MNRAS*, 321, 372
- Labbé, I., van Dokkum, P., Nelson, E., et al. 2022, arXiv:2207.12446
- Linden, S., & Virey, J.-M. 2008, *PhRvD*, 78, 023526
- Linder, E. V. 2003, *PhRvL*, 90, 091301
- Linder, E. V. 2005, *PhRvD*, 72, 043529
- Linder, E. V. 2006, *PhRvD*, 73, 063010
- Linder, E. V., & Cahn, R. N. 2007, *Aph*, 28, 481
- Maggiore, M., & Riotto, A. 2010, *ApJ*, 717, 515
- Mainini, R., Maccio, A. V., Bonometto, S. A., & Klypin, A. 2003, *ApJ*, 599, 24
- Mehrabi, A. 2018, *PhRvD*, 97, 083522
- Menci, N., Grazian, A., Castellano, M., et al. 2020, *ApJ*, 900, 108
- Pace, F., Waizmann, J.-C., & Bartelmann, M. 2010, *MNRAS*, 406, 1865
- Peebles, P. J. E. 1993, *Principles of Physical Cosmology* (Princeton, NJ: Princeton Univ. Press)
- Peebles, P. J. E., & Ratra, B. 1988, *ApJ*, 325, L17
- Planck Collaboration, Aghanim, N., Akrami, Y., et al. 2020, *A&A*, 641, A6
- Press, W. H., & Schechter, P. 1974, *ApJ*, 187, 425
- Risaliti, G., & Lusso, E. 2019, *NatAs*, 3, 272
- Ryan, E., Stark, D. P., Whitler, L., et al. 2022, arXiv:2208.14999
- Sangwan, A., Mukherjee, A., & Jassal, H. K. 2018, *JCAP*, 01, 018
- Santini, P., Ferguson, H. C., Fontana, A., et al. 2015, *ApJ*, 801, 97
- Scherrer, R. J. 2015, *PhRvD*, 92, 043001
- Sheth, R. K., & Tormen, G. 1999, *MNRAS*, 308, 119
- Steinhardt, C. L., Kokorev, V., Rusakov, V., et al. 2022, arXiv:2208.07879
- Tinker, J., Kravtsov, A. V., Klypin, A., et al. 2008, *ApJ*, 688, 709
- Treu, T., Roberts-Borsani, G., Bradac, M., et al. 2022, *ApJ*, 935, 110
- Wang, Q., Gao, L., & Meng, C. 2022, arXiv:2206.06313
- Warren, M. S., Abazajian, K., Holz, D. E., & Teodoro, L. 2006, *ApJ*, 646, 881